

Original Research

# Proteomic Landscape Associated with Cognitive Impairment in Individuals with Long-term Methamphetamine Dependence

Xuru Wang<sup>1</sup>, Liangtao Li<sup>2</sup>, Hongbiao Wang<sup>3</sup>, Yu Zhou<sup>1</sup>, Yongchao Li<sup>4</sup>, Cuicui Li<sup>5</sup>, Chenglin Zhou<sup>1</sup>, Yingying Wang<sup>1,\*</sup>

Academic Editors: George Panagis and Gernot Riedel

Submitted: 4 December 2023 Revised: 5 January 2024 Accepted: 15 January 2024 Published: 24 May 2024

#### **Abstract**

Background: Methamphetamine (METH) is a highly addictive drug that directly affects the central nervous system. METH use not only harms the user's health but also poses risks and costs to society. Prolonged METH dependence has been shown to impair cognition, which may be the primary factor in impulsive drug-seeking behaviors and high relapse rates. However, the molecular mechanisms underlying METH addiction and METH-induced cognitive decline remain poorly understood. Methods: To illuminate the potential molecular mechanisms underpinning METH addiction, we compared serum protein expression levels between 12 long-term METH users and 12 healthy controls using label-free quantitative proteomics. Bioinformatic analyses were conducted to determine functional networks and protein-protein interactions. Results: In total, 23 differentially expressed proteins were identified between the two groups. The differentially expressed proteins were related to cognitive dysfunction, neuroinflammation, immune impairment, metabolic disturbances, and calcium binding and regulation. Conclusions: These 23 proteins may underpin the multi-system damage induced by chronic METH exposure. Our findings provide novel insights into the molecular basis of METH addiction and inform potential prevention and treatment strategies for individuals with METH dependence.

Keywords: METH; label-free proteomics; bioinformatic analyses; addiction; cognitive disorder; molecular mechanism

# 1. Introduction

Methamphetamine (METH) is a highly addictive psychostimulant drug that causes euphoria and arousal. Originally used as an anti-fatigue and diet aid, METH is now recognized to have dependence-forming properties and is classified as a Schedule II controlled substance by the USA Food and Drug Administration (Scheduling of Controlled Substances: Placement of Methamphetamine into Schedule II. Federal Register) [1]. Due to easy access to its components and simple manufacturing process, alongside its strong rewarding effects, METH is used as an illicit drug globally, causing substantial individual and societal harm [2]. It is noteworthy that due to the highly addictive nature of METH, prolonged use of this substance significantly increases the likelihood of developing an addiction. Therefore, in this manuscript, the terms 'METH addiction' and 'prolonged/long-term METH use/dependence' are employed interchangeably for the sake of conceptual coherence and effective paraphrasing.

Prolonged METH use damages both health and cognition [3]. The chronic effects of METH elicit hyperactivity in the central nervous system (CNS) by elevating extracel-

lular dopamine, serotonin, and norepinephrine [4]. Longterm METH exposure may result in significant cognitive impairments [3]. A meta-analysis found that individuals addicted to METH have significant deficits in impulsive behavior, reward processing, and social cognition processes [3]. Attention, executive function, speech, learning, memory, visual memory, and working memory processes are also mildly impaired [3]. A comprehensive review incorporating numerous neuroimaging studies revealed that individuals with METH dependence exhibit various abnormalities in brain activity. These abnormalities are primarily observed in the prefrontal cortex and striatum, areas that are essential for cognitive flexibility, inhibitory control, and decision-making [5]. Those cognitive deficits likely contribute to the impulsive drug-seeking behavior of METH users. Due to the legal prohibition of METH use in many countries, such as China, testing cognitive function in active METH users raises significant ethical concerns. Consequently, most studies exploring the molecular mechanisms underlying METH-induced cognitive dysfunction have predominantly utilized animal models. Rodent studies have shown that chronic METH exposure damages brain struc-

<sup>&</sup>lt;sup>1</sup>School of Psychology, Shanghai University of Sport, 200438 Shanghai, China

<sup>&</sup>lt;sup>2</sup>Department of Sports, Suzhou Vocational University, 215000 Suzhou, Jiangsu, China

<sup>&</sup>lt;sup>3</sup>Department of Physical Education, Shanghai University of Medicine & Health Sciences, 201318 Shanghai, China

<sup>&</sup>lt;sup>4</sup>Xiangcheng Administration Center, 215000 Suzhou, Jiangsu, China

<sup>&</sup>lt;sup>5</sup>Department of Neurobiology, Affiliated Mental Health Center and Hangzhou Seventh People's Hospital, Zhejiang University School of Medicine, 310058 Hangzhou, Zhejiang, China

<sup>\*</sup>Correspondence: wangyingving@sus.edu.cn (Yingying Wang)

ture and function by disrupting the blood-brain barrier, eliciting neuroinflammation, impairing neuron formation and differentiation [6], and altering gene expression [7,8].

Prolonged METH exposure also enhances amyloid precursor protein (APP) expression, indicative of the neurodegenerative changes observed in Alzheimer's disease (AD) and Parkinson's disease (PD) [9,10]. In rats, chronic METH exposure leads to emotional disorders and impulsive drug-seeking behavior associated with prefrontal cortical dopamine depletion and decreased striatal dopamine transporters [10]. Dopaminergic deficits persist even after prolonged withdrawal, suggesting potential long-term impacts on cognitive function [10].

Given the significant impact of the dopaminergic system in METH-induced cognitive effects, it is crucial to recognize METH's extensive influence on a broader spectrum of biological pathways [11]. An illustrative example of this is the damage that METH inflicts on midbrain dopamine neurons, leading to the release of neuroinflammatory agents like nuclear factor kappa-light-chain-enhancer of activated B cells (NF- $\kappa$ B) [12,13]. A study focusing on three common immune cell lines revealed that METH exposure leads to distinct expression patterns at the mRNA level, thereby contributing to an increased incidence of infectious diseases [14]. Moreover, METH usage is associated with heightened inflammatory and oxidative stress markers, as evidenced by the rise in blood C-reactive protein levels [15]. Such widespread effects underscore the necessity of employing proteomic methodologies, particularly label-free proteomics, for a comprehensive understanding of METH's multifaceted impact, which transcends the confines of neurotransmitter systems.

Proteomic approaches, especially the label-free technique, offer an expansive framework for elucidating METH's complex mechanisms. This sophisticated method facilitates in-depth analysis of proteomic changes associated with METH use, potentially uncovering diverse biological pathways that contribute to cognitive deterioration and the development of addictive behaviors [11]. The central hypothesis of this study is that prolonged METH exposure leads to substantial alterations in serum proteomic profiles, reflecting not only disruptions in neurotransmitter function but also a range of biological processes integral to the pathophysiology of addiction and cognitive impairment.

Although the dopamine reward system appears to mediate METH addiction in part, the specific mechanisms underpinning addiction remain unclear [16,17]. Proteomic analyses enable exploration of the mechanisms of drug dependence. Label-free proteomics quantitatively analyzes differences in protein expression between samples and has been widely used in neuroscientific research. Compared with labeling techniques, this technology is more costeffective, sensitive, and accurate.

Thus, in the present study, we used label-free proteomics to compare serum protein profiles between long-

term METH users and healthy controls. This systems-level analysis aimed to investigate the potential molecular mechanisms of METH addiction and the associated cognitive decline. Our findings shed light on the molecular underpinnings of METH dependence, revealing a comprehensive profile of serum proteins that are differentially expressed in individuals with METH dependence. In addition, these results offer novel insight into the multi-systemic nature of METH's adverse effects and may guide the design of comprehensive treatment strategies that address both the addiction and its widespread health implications.

#### 2. Materials and Methods

# 2.1 Participants

This study was approved by the Ethics Committee of Shanghai University of Sport (No. 102772019RT044) and conducted in accordance with the Helsinki Declaration of 1975. All participant information remained confidential and all patients provided written informed consent. Twelve individuals with METH dependence were recruited from compulsory detoxification programs in Zhejiang province, China. Twelve control subjects were recruited from the community within Changhai Street, Yangpu District, Shanghai. These participants were selected according to the following criteria: (1) men aged 18-45 years; (2) with long-term use of METH (2 or more years); (3) confirmed to meet the criteria for methamphetamine dependence as outlined in the DSM-V (Diagnostic and Statistical Manual of Mental Disorders, Fifth Edition) based on the Structured Diagnostic Interview [18]; (4) without a serious infectious disease, autoimmune disease, severe mental illness, neurological disease, Human Immunodeficiency Virus (HIV) infection, obvious disease that would affect organ quality, hypertension, hyperlipidemia, diabetes, tumor, or other disease; (5) without use of nonamphetamine-type drugs; and (6) without consumption of pharmaceutical drugs, cocaine-like substances, alcohol, or tobacco within 2 weeks of serum sampling. The METHdependent group had a mean age of 29.83 years (standard deviation [SD] = 5.80 years), an average duration of drug use spanning 4.18 years (SD = 1.40 years), a typical weekly drug usage frequency of 2.21 times (SD = 1.94 times), and a mean quantity of 0.265 g per drug consumption event (SD = 0.11 g). Participants in the control group were 12 healthy men (mean age 32.58 years, SD = 6.32 years) who met the same criteria as the METH-dependent group, except without history of drug misuse. The 12 control participants were randomly assigned to one of three subgroups (A, B, or C), with four participants in each subgroup. Similarly, the 12 participants with METH dependence were randomly assigned to one of three subgroups (D, E, or F), with four participants in each subgroup.



# **Hierarchy Clustering**

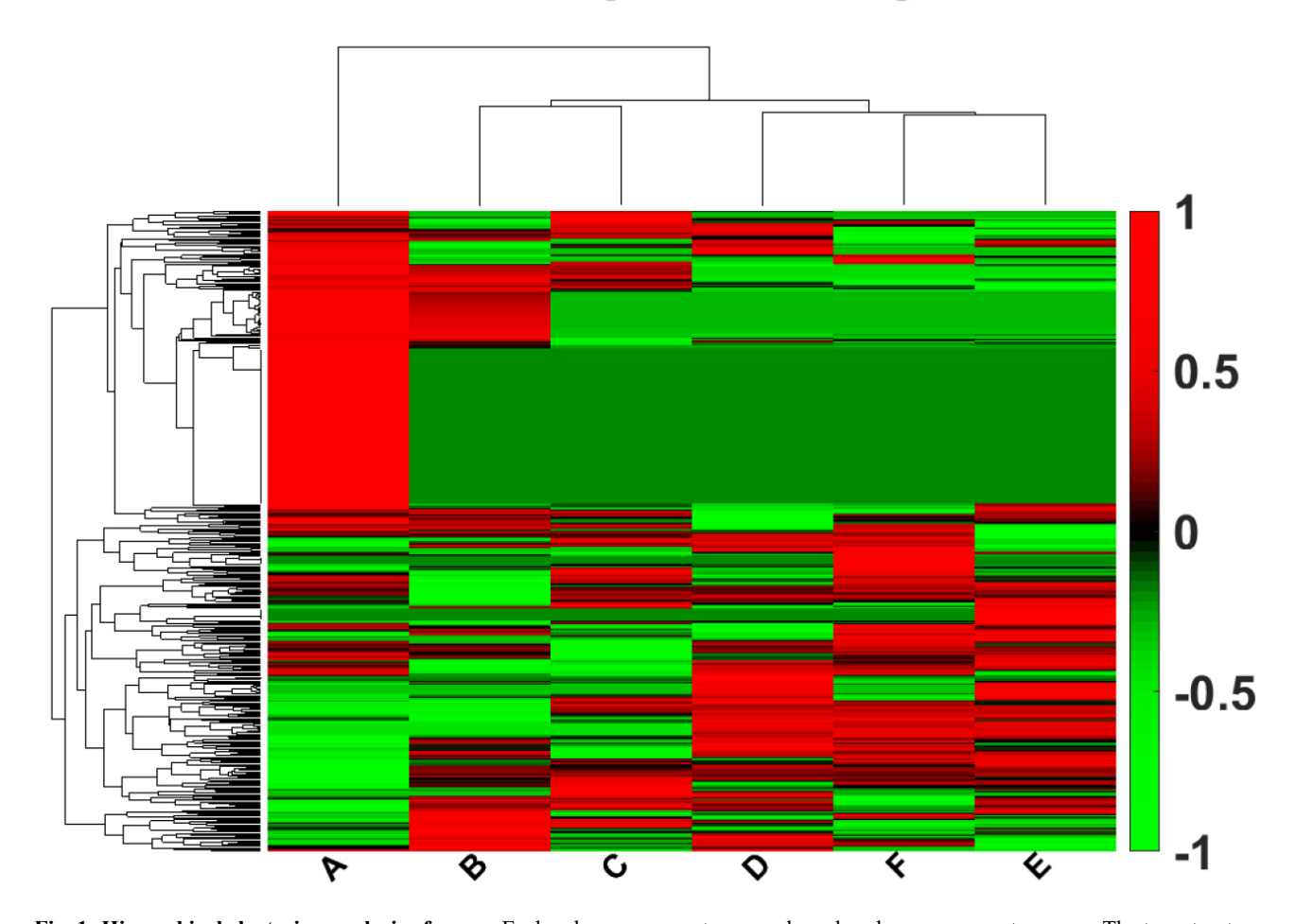


**Fig. 1. Hierarchical clustering analysis of genes.** Each column represents a sample and each row represents a gene. The tree structure above the colored area represents the clustering of similarity between samples, and the tree structure on the left represents the clustering of similarity between genes. Red indicates a high level of expression, and green indicates a low level of expression. Letters along the x-axis indicate the participant group. Along the y-axis, positive numbers indicate upregulation and negative numbers indicate downregulation.

# 2.2 Serum Sample Preparation

Fasting venous blood samples (5 mL) were drawn from the 24 participants and clotted at 4 °C for 30 min. The samples were then centrifuged at 1000 ×g for 10 min, then the supernatants were collected. The samples were subgrouped as described above to create a total of six serum samples (A, B, C, D, E, and F). Albumin and Immunoglobulin G (IgG) Depletion SpinTrap columns (No. 28-9480-20, GE Healthcare, Buckinghamshire, UK) were used, and the manufacturer's instructions were followed to remove the high-abundance proteins from the serum. The total protein concentration was then determined using a Pierce<sup>TM</sup> Coomassie (Bradford) Protein Assay Kit (Cat. No. 23200, Thermo Fisher Scientific, Rockford, IL, USA).

# 2.3 Proteolysis and Peptide Purification

Sodium dodecyl sulfate-polyacrylamide gel electrophoresis was used to separate the proteins in the serum

sample (40 µg/sample). The gels were cut and the pieces were washed twice with double-distilled water. Silver dye decolorizer (equal volumes of 100 mmol/L sodium thiosulfate (Thermo Fisher Scientific, Fair Lawn, NJ, USA) and 30 mmol/L potassium ferricyanide (Thermo Fisher Scientific, Fair Lawn, NJ, USA)) was used to destain the gel, which was then washed twice with water. Acetonitrile was used to dehydrate the gel fractions. The reducing reagent (dithiothreitol, I1149-25G, 10 mmol/L, SIGMA, Saint Louis, MO, USA) was allowed to react for 1 h at 37 °C with the gel fractions, which were then dehydrated with acetonitrile. A cysteine blocking reagent (iodoacetamide, 25 mmol/L, Thermo Fisher Scientific, Fair Lawn, NJ, USA) was added and reacted with the gel fractions for 30 min at room temperature in the dark. The fractions were washed twice and dehydrated. The gel pieces were then digested using trypsin (V5113, Promega, Madison, WI, USA) overnight at 37 °C. An acetonitrile (50%) and trifluoroacetic acid (0.1%) solution (400 µL) was added and incubated at 37 °C for 30 min.



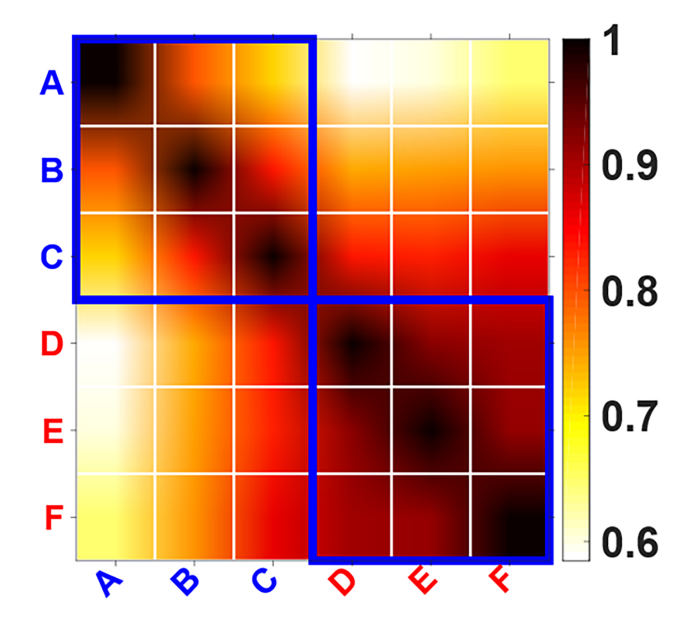


**Fig. 2.** Correlation analysis of the samples. The ordinate and abscissa represent the six samples: A, B, C, D, E, and F. The color depth represents the degree of correlation between the samples as indicated in the color bar.

This step was repeated twice. Finally, the eluates from each respective sample were combined, and the peptides were desalted and freeze dried.

#### 2.4 Liquid Chromatography–Mass Spectrometry Analysis

The peptides were analyzed using an Orbitrap Fusion Lumos Tribrid (Thermo Fisher Scientific, San Jose, CA, USA) mass spectrometer using a chromatographic column (ChromXP, C18, 3 µm, 120 Å; catalog No. 805-00120, SCIEX, Framingham, MA, USA). A binary solvent system composed of water containing buffer A (0.1% formic acid and 2% acetonitrile in water) and buffer B (98% acetonitrile and 0.1% formic acid) was used for liquid chromatography. The peptides were separated by a gradient of buffer B (5% B, 0–5 min; linearly increasing concentrations of 5%–40% B within 100 min; increased to 80% B in 1 min and washed for 5 min; decreased to 5% B in 1 min and isocratic at 5% B for 13 min). The solvent system flow rate was 300 nL/min. The mass spectrometer was operated in the scan range of 300-1400 m/z, with a spray voltage at 2500 V and a dynamic exclusion time of 12 s. All data were acquired using "high-low" mode, in which during a maximum 3-s cycle time, the most abundant multiply-charged parent ions were selected with high resolution (120,000 at m/z 200) from the full scan for higher-energy collisional dissociation fragmentation. Precursor ions with singly charged and charge states over 7 were excluded. The target value for the second mass spectrometry (MS2) spectra was set at 5000 (the automated gain control was enabled with a maximum injection time of 35 ms), the isolation window was set to 1.6 m/z, and 35% was used for the normalized collision energy. Data were

acquired using Xcalibur software 4.1 (Thermo Fisher Scientific, Waltham, MA, USA) [19].

# 2.5 Bioinformatic Analysis

All mass-spectrometric data were analyzed using MaxQuant 1.5.2.8 (University of Halle-Wittenberg, Halle, Germany; https://www.maxquant.org) [20] against the human UniProt FASTA database (https://www.uniprot.org/proteomes/UP000005640). Carbamidomethyl cysteine was searched as a fixed modification, and oxidized methionine and protein N-terminal acetylation as variable modifications. Enzyme specificity was set to trypsin/P. Two missing cleavage sites were allowed. For mass spectrometry and tandem mass spectrometry, the tolerance of the main search for peptides was set at 7 ppm and 20 ppm, respectively. The peptide, protein, and site false discovery rates were fixed at a significance level not greater than 0.01. Label-free protein quantitation was performed with a minimum ratio count of 2.

Quantitative data for the detected proteins were analyzed using MetaboAnalyst software 5.0 (McGill University, Montreal, Canada; https://www.metaboanalyst.ca) [21]. Proteins were removed from further analysis if the detection values were missing in more than 50% of the samples from either the METH-dependent or control group or if the quantitative values were consistent across all samples.

For proteins with missing quantitative values, missing values were imputed as one-half the minimum positive value in the original data using the minimum fill method. To obtain normalized protein abundance data for subsequent analyses, the summed intensity values for all proteins measured in each sample were calculated, and individual protein intensities within a sample were divided by the sample's total intensity value. Hierarchical clustering analysis and visualization of the acquired protein profiles for all samples and genes were performed using Multiple Array Viewer software 4.9.0 (Agilent Technologies, Santa Clara, CA, USA; https://webmev.tm4.org) [22]. Principal component analysis of the proteins was carried out using MAT-LAB software R2019b (MathWorks, Natick, MA, USA; https://www.mathworks.com) [23]. The orthogonal partial least squares discriminant analysis was performed using SIMCA software 14.1 (Umetrics, Umeå, Sweden; https: //www.sartorius.com/en/products/process-analytical-techn ology/data-analytics-software/mvda-software/simca) [24].

To identify proteins with significantly different expression between METH-dependent and control groups, Statistical Package for the Social Sciences (SPSS, 24.0) (International Business Machines Corporation, Armonk, NY, USA; https://www.ibm.com/products/spss-statistics) software [25] was utilized. A threshold filter requiring at least a two-fold change in the protein ratio between groups and a *p*-value < 0.05 was applied. Gene Ontology (GO) and Kyoto Encyclopedia of Genes and Genomes (KEGG) pathway analyses were conducted using the Database for Anno-



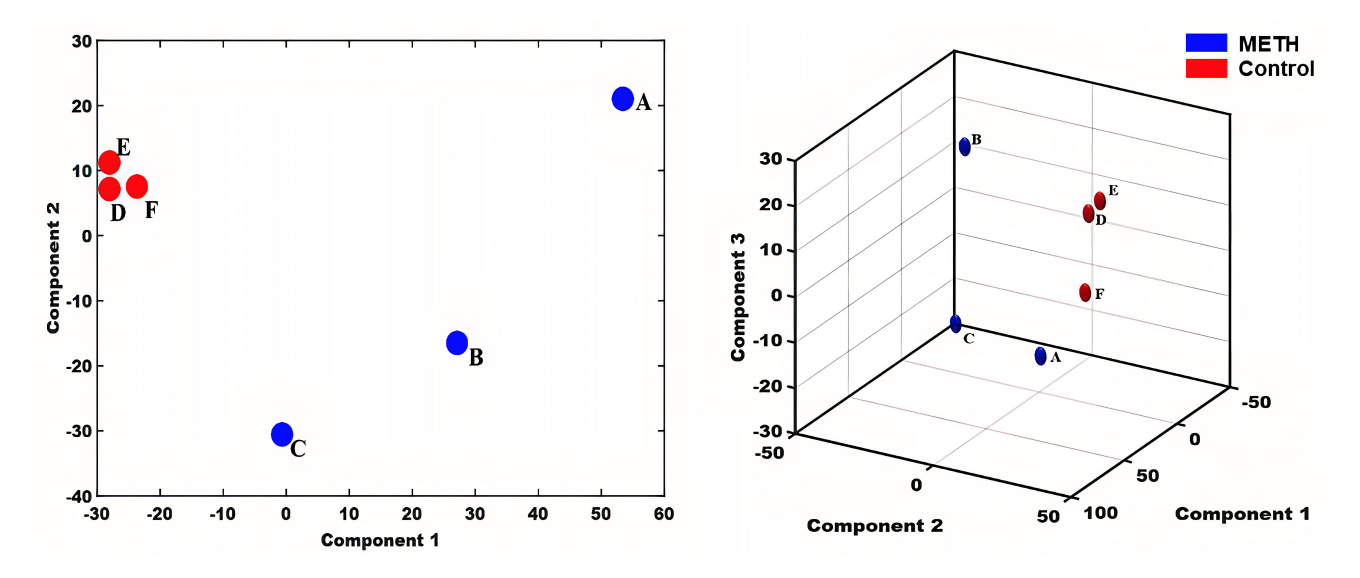


**Fig. 3. Principal Component Analysis.** Letters indicate the participant group, with A, B, and C representing samples from healthy individuals and D, E, and F representing samples from individuals with methamphetamine dependence. METH, methamphetamine.

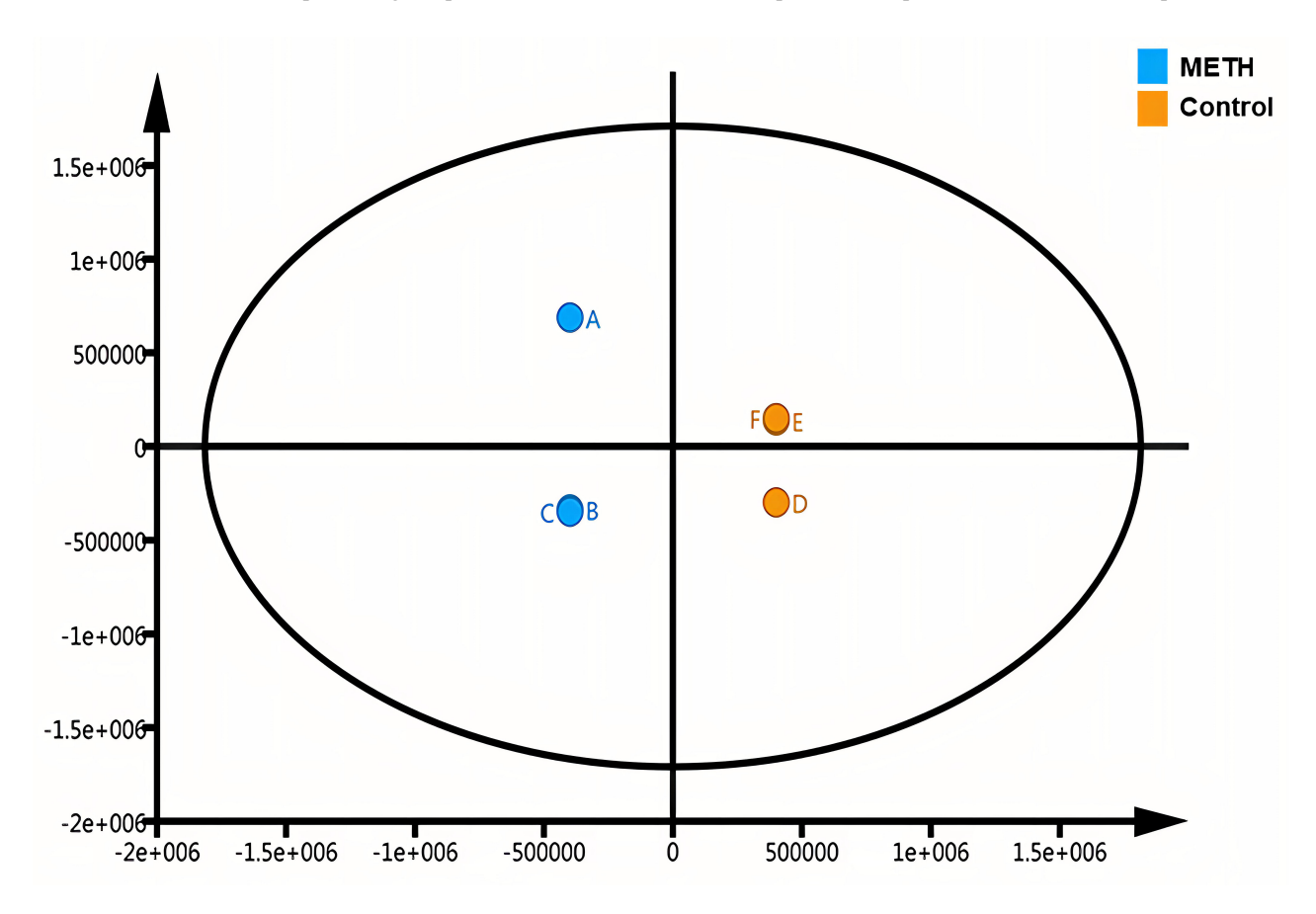


**Fig. 4. Orthogonal partial least squares discriminant analysis.** Letters indicate the participant group, with A, B, and C representing samples from healthy individuals and D, E, and F representing samples from individuals with methamphetamine dependence.

tation, Visualization and Integrated Discovery. A general pathway and network analysis was performed with Ingenuity Pathway Analysis (IPA) software (QIAGEN, Hilden, Germany; https://digitalinsights.qiagen.com/IPA) [26].

#### 3. Results

3.1 Proteins Identified by Mass Spectrometry in METH-dependent and Healthy Control Groups

A total of 459 proteins were identified by proteomic workflow, and 308 proteins with quantitative information



were finally obtained using MetaboAnalyst software analysis (Supplementary Table 1). We used the Multiple Array Viewer software to perform hierarchical clustering analysis at both the sample- and gene-levels of those 308 proteins (Fig. 1). The clustering results indicated that the protein expression profiles of the METH-dependent group samples (D, E, and F) exhibited a high degree of resemblance, suggesting that these samples share a closely related pattern of protein expression. Similarly, the protein expression profiles within the control group samples (A, B, and C) displayed a substantial similarity, reflecting a consistent pattern of expression distinct from the METH-dependent group. This similarity, as evidenced by the proximity of the samples to one another on the dendrogram and the homogeneity in expression levels represented by the color coding on the heat map, underscores the comparative analysis of gene expression levels within each group. Significant differences in the protein expression profiles were observed between the two sets of groups. Correlation analysis of the samples showed high intragroup correlation but low intergroup correlation between the METH-dependent and control groups (Fig. 2).

We used MATLAB software to perform two- and three-dimensional principal component analyses of the 308 proteins (Fig. 3) and completed the orthogonal partial least squares discriminant (OPLS) analysis using SIMCA software (Fig. 4). Both the principal component analysis and OPLS results indicated close clustering of samples within the same group and a clear separation between METH-dependent and control groups based on protein expression levels.

# 3.2 Screening and Functional Analysis of Differentially Expressed Proteins (DEPs)

#### 3.2.1 Screening of DEPs

To identify differentially expressed proteins (DEPs) between the METH-dependent and control groups, a threshold filter requiring at least a two-fold change in expression ratio and a value of p < 0.05 was applied. This analysis found 23 significant DEPs (Figs. 5,6, and Table 1). Compared with the control group, the METH-dependent group displayed decreased expression of four proteins but increased expression of 19 proteins.

#### 3.2.2 GO Analysis of DEPs

GO analysis provides a standardized system for functional characterization of genes and gene products using controlled vocabulary terms. A GO analysis consists of three structured ontologies that describe cellular components (location), molecular functions, and biological processes. We performed a GO analysis for DEPs between the METH-dependent and control groups. The results indicated the predominant subcellular localizations (Fig. 7A), molecular functions (Fig. 7B), and biological processes (Fig. 7C) associated with the DEPs. In brief, the majority of DEPs lo-

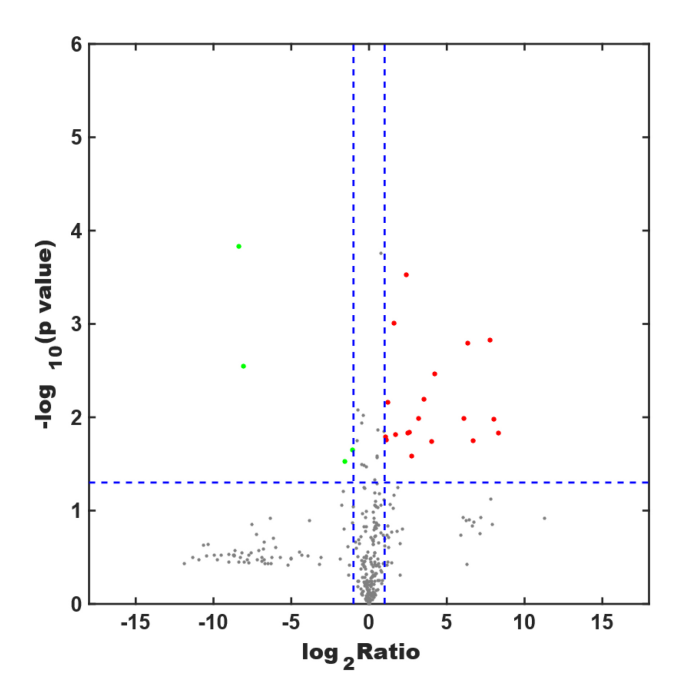


Fig. 5. Screening for differentially expressed proteins. The x-axis shows the logarithm of the ratio of protein expression between the METH-dependent and control groups, and the y-axis shows the p value. Each dot in the figure represents a protein. A red dot is a highly expressed protein, whereas a green dot is a protein with low expression. Gray dots represent proteins with expression levels that do not differ between the two groups.

calized to eight cellular components, performed seven key molecular functions, and participated in 10 major biological processes.

# 3.2.3 KEGG Metabolic Pathway Analysis

A KEGG pathway analysis was conducted to analyze enriched metabolic and signaling pathways among the DEPs. The results showed that the top two metabolic pathways were the extracellular matrix (ECM)–receptor interaction pathway (Fig. 8, Ref. [27]) and the hematopoietic cell lineage signaling pathway (Fig. 9, Ref. [27]). The ECM–receptor interaction pathway was enriched in DEPs that included platelet glycoprotein V and cartilage oligomeric matrix protein thrombospondin. The hematopoietic cell lineage pathway contained colony stimulating factor 1 receptor (CSF1R) CD115 and the platelet glycoprotein V (CD42) DEPs.

#### 3.2.4 IPA

IPA provides a comprehensive analysis of proteomic data to elucidate protein expression mechanisms and related biological processes, such as post-translational modifications, signaling pathways, protein interactions, and differential protein signatures.



Table 1. Information on differentially expressed proteins.

Entry	Entry name	Gene name	Ratio (METH/Control)	Log2 (Ratio)	p value	Sig (METH/Control)
A0A075B6K0	LV316_HUMAN	IGLV3-16	0.003025	-8.36868	0.000149	-1
A0A075B6Q	HV364_HUMAN	IGHV3-64	0.476451	-1.0696	0.022344	-1
A0A0C4DH72	KV106_HUMAN	IGKV1-6	9.177759	3.198142	0.010307	1
O43300	LRRT2_HUMAN	LRRTM2,	104.4256	6.706332	0.017745	1
		KIAA0416, LRRN2				
O75636	Ficolin-3_HUMAN	Ficolin-3, FCNH,	2.058334	1.041477	0.01615	1
		HAKA1				
P01717	LV325_HUMAN	IGLV3-25	0.003759	-8.05539	0.002862	-1
P01721	LV657_HUMAN	IGLV6-57	11.47183	3.520024	0.006416	1
P01833	PIGR_HUMAN	PIGR	5.182036	2.373519	0.000298	1
P02745	C1QA_HUMAN	C1qA	18.68545	4.223843	0.003406	1
P05067	A4_HUMAN	APP, A4, AD1	219.4922	7.778026	0.00148	1
P05109	S10A8_HUMAN	S100A8, CAGA,	6.596966	2.721803	0.025996	1
		CFAG, MRP8				
P07195	LDHB_HUMAN	LDHB	2.318441	1.213155	0.006908	1
P07333	CSF1R_HUMAN	CSF1R, FMS	5.604841	2.486673	0.014825	1
P0DJI8	SAA1_HUMAN	SAA1	316.1776	8.304592	0.014613	1
P0DOX3	IGD_HUMAN		3.064636	1.615716	0.000975	1
P0DOX6	IGM_HUMAN		3.263239	1.706304	0.015359	1
P11597	CETP_HUMAN	CETP	263.3256	8.040704	0.010555	1
P27487	DPP4_HUMAN	DPP4, ADCP2,	67.86644	6.084626	0.010224	1
		CD26				
P33151	CADH5_HUMAN	CDH5	2.13414	1.093655	0.017554	1
P40197	GPV_HUMAN	GP5	80.28949	6.327139	0.001601	1
P49747	COMP_HUMAN	COMP	16.36481	4.032525	0.018041	1
Q12805	FBLN3_HUMAN	EFEMP1, FBLN3,	6.012555	2.587978	0.014533	1
		FBNL				
Q9HDC9	APMAP_HUMAN	APMAP, C20orf3,	0.34513	-1.53479	0.029935	-1
		UNQ1869/PRO4305				

METH indicates methamphetamine; Sig indicates differential protein expression between the control (A, B, and C) and METH (D, E, and F) group samples, with sig = 1 representing an upregulated protein and sig = -1 representing a downregulated protein. For the full names of the differentially expressed proteins, please refer to the supplementary information.

# 3.2.5 Signal Pathway Enrichment Analysis

Significant pathway enrichment analysis using IPA identified key metabolic and signaling pathways enriched with the DEPs between the METH-dependent and control groups (Fig. 10). Major DEPs involved in those pathways were serum amyloid A-1 (SAA1), S100A8, cholesterol ester transfer protein (CETP), dipeptidyl peptidase 4 (DPP4), APP, L-lactate dehydrogenase B chain (LDHB), colonystimulating factor 1 receptor (CSF1R), and C1q subcomponent subunit A (C1qA).

#### 3.2.6 Functional Enrichment Analysis

We used IPA software and the Ingenuity Knowledge Base to perform biological function and disease analyses (Fig. 11A) as well as toxicological analysis (Fig. 11B) for the DEPs. The results demonstrated that the DEPs were predominantly associated with cellular movement, immunity, inflammatory response, the blood system, cell assembly and tissue, cell morphology, neurological diseases, in-

tercellular signals and interactions, connective tissue diseases, and cardiovascular system development and function.

# 3.2.7 Protein Interaction Network Analysis

The IPA showed that the DEPs were enriched in five protein interaction networks (Fig. 12). The network shown in Fig. 12A that is related to cellular assembly/organization, metabolic disease, and cellular movement contained DEPs, APP, SAA1, DPP4, leucine-rich repeat transmembrane neuronal protein 2 (LRRTM2), cartilage oligomeric matrix protein (COMP), calcium-binding protein S100A8, polymeric immunoglobulin receptor (PIGR), macrophage CSF1R, LDHB, and cadherin-5 (CDH5). The network shown in Fig. 12B that is associated with lipid metabolism, molecular transport, and small molecule biochemistry included DEPs, CETP and complement C1qA. The network shown in Fig. 12C that is linked to immune response, inflammatory response, and cardiovascular disease



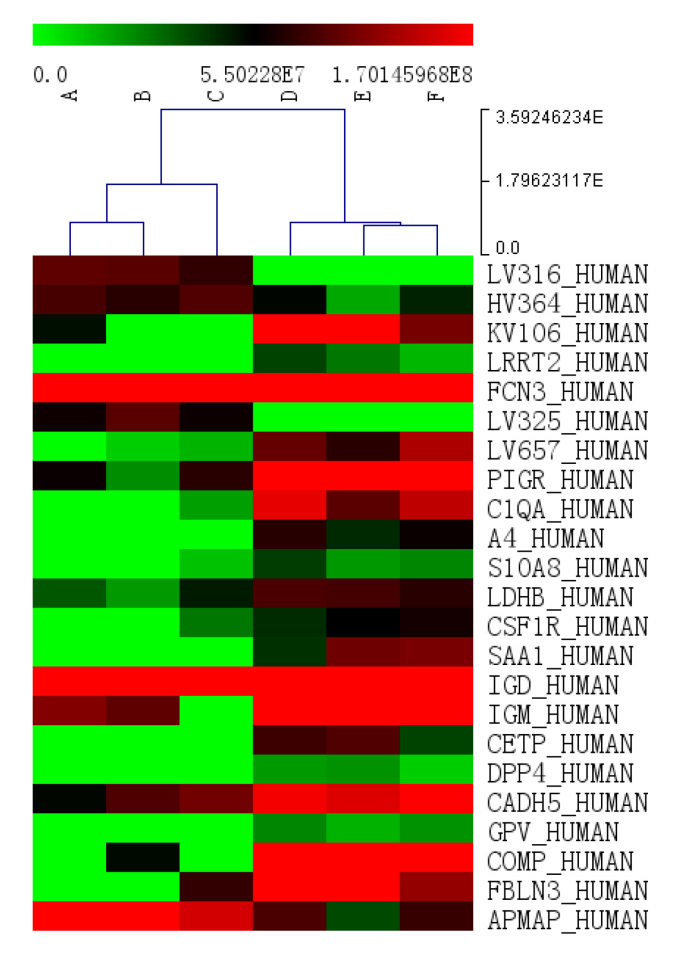


**Fig. 6.** Cluster analysis of differentially expressed proteins. Each column represents a sample and each row represents a named gene. The tree structure above the colored area represents the clustering of similarity between samples. Red indicates a high level of expression, whereas green indicates a low level of expression.

involved the DEP ficolin-3. DEP glycoprotein V (GP5) is part of the network shown in Fig. 12D, which is related to connective tissue disorders, hematological disease, and organismal injury and abnormalities. Epidermal growth factor-containing fibulin-like extracellular matrix protein 1 (EFEMP1) was the DEP involved in the network shown in Fig. 12E, which was associated with cellular growth, proliferation, cancer, and organismal injury and abnormalities.

# 4. Discussion

METH is a potent CNS stimulant that elicits euphoria and pleasure through activation of the brain's reward pathway [3]. However, chronic use leads to dependence, addiction, and adverse health effects, including of the nervous, cardiovascular, cerebrovascular, and immune systems [4,5].

The present study utilized a proteomics approach to identify differentially expressed serum proteins between individuals with METH dependence and healthy control individuals. In total, 23 proteins were significantly altered,

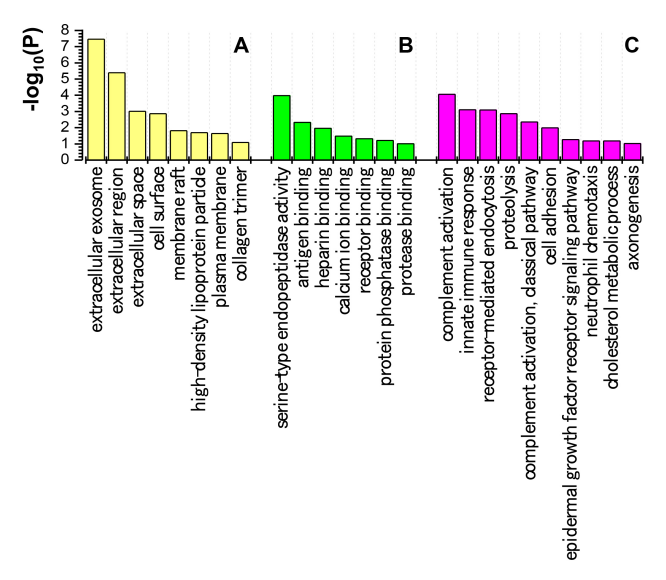


Fig. 7. Gene ontology analysis of proteins differentially expressed between methamphetamine-dependent and healthy control individuals. (A) Locations of differentially expressed proteins. (B) Molecular functions of the differentially expressed proteins. (C) Biological processes that the differentially expressed proteins participate in. The ordinate (P) represents the degree of enrichment.

with four downregulated and 19 upregulated proteins in the METH-dependent group compared with the control group. In-depth bioinformatic analyses indicated that these DEPs participated in pathways and processes related to cognitive disorder, neuron impairment, immune response, energy metabolism, and calcium binding or regulation. This proteomics profile provides insights into the biological impact at the protein level of METH addiction and misuse.

#### 4.1 Cognitive Disorder-related Proteins

The misuse of METH has been associated with cognitive impairment, including AD [28], a neurodegenerative disorder characterized by amyloid beta  $(A\beta)$  plaques, neuronal death, and memory decline [29]. In the present study, we found DEPs in long-term METH users related to  $A\beta$  accumulation and AD pathology, including APP, SAA1, CETP, and adipocyte serum membrane-associated protein (APMAP).

APP is a single transmembrane neuronal protein widely distributed in tissues and concentrated at neuronal synapses [30]. APP can be cleaved into different fragments by  $\alpha$ -,  $\beta$ -, or  $\gamma$ -protease, including cleavage by  $\beta$ - and  $\gamma$ -protease that generates A $\beta$  [31]. As the precursor of A $\beta$ , APP is implicated in early neuronal damage, but may also have positive protective roles in cell adhesion, maintaining synaptic membrane stability, inhibiting serine protease activity, and participating in the immune response of the CNS [32]. Our results showed an elevated expression of APP in individuals with METH dependence, suggesting increased



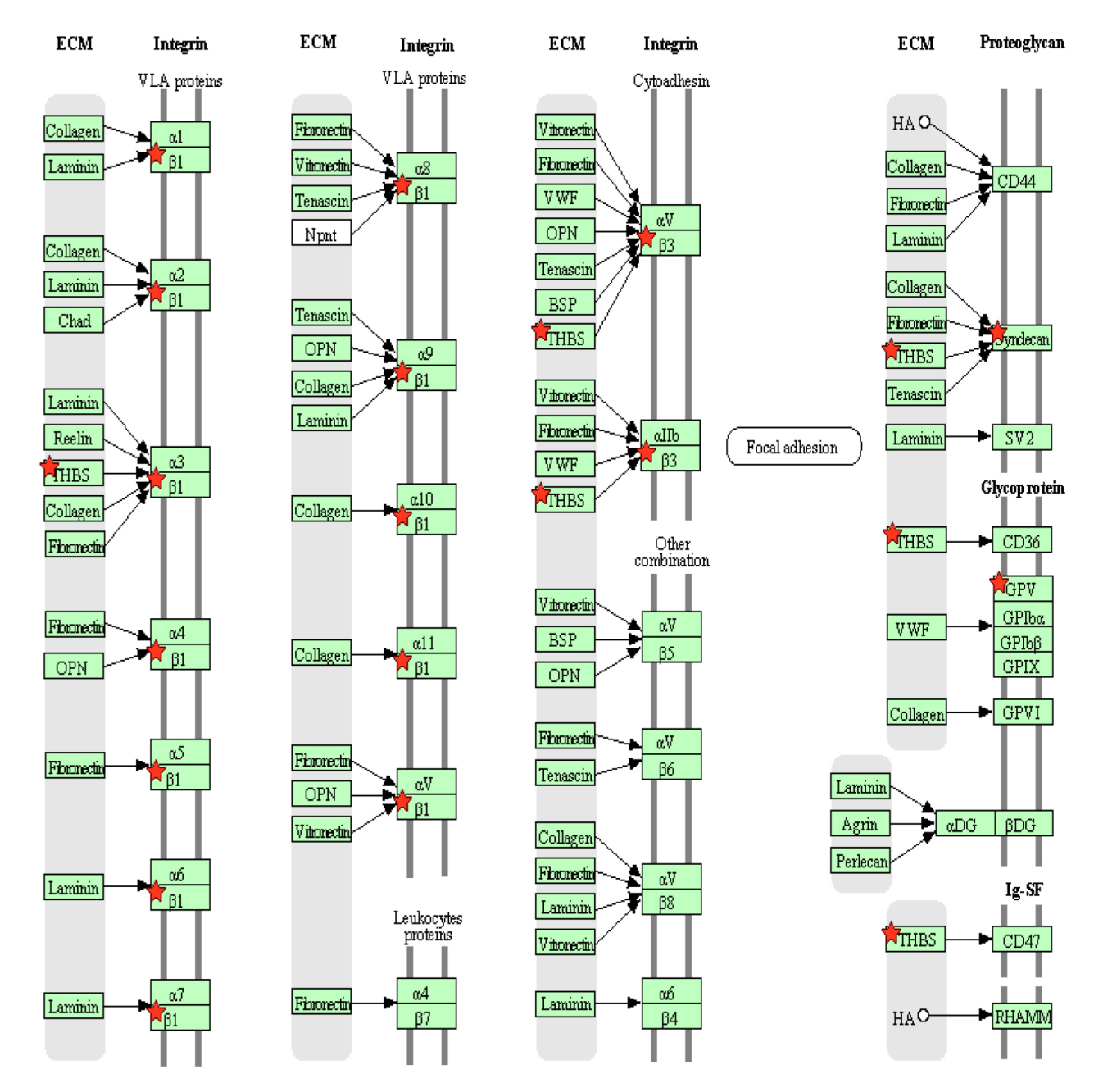


Fig. 8. Differentially expressed proteins are involved in the extracellular matrix (ECM)-receptor interaction pathway. Red stars represent the identified differentially expressed proteins. GPV, platelet glycoprotein V; HA, hemagglutinin; THBS, thrombospondin; VLA, very late antigen. The information about all abbreviations can be found at: https://www.genome.jp/pathway/hsa04512 [27].

risk of  $A\beta$  plaque formation and neurodegeneration. These results are consistent with previous studies, which suggest METH abuse is related to types of cognitive decline such as deficits in cognitive control, decision-making, and social skills [33], all of which are clinical symptoms of AD [34].

CETP promotes cholesterol transfer from high-density lipoprotein to low-density lipoprotein or very low-density lipoprotein, which may be associated with atherosclerosis. Intracellular cholesterol accumulation also stimulates  $A\beta$  production [35]. The high expression of CETP in chronic METH users in the present study suggests heightened risks

of cardiovascular disease and A $\beta$ -associated neurodegenerative diseases.

APMAP is a membrane protein ubiquitously expressed in various tissues and organs, where it promotes pre-adipocyte differentiation into mature adipocytes to maintain normal physiological metabolism of fat cells. Studies have shown that inhibition of APMAP expression destabilizes APP and increases  $A\beta$  production [36]. The present study found decreased serum APMAP protein in METH users compared with healthy controls, which may lead to an increase in the level of  $A\beta$  to thereby increase the risk of neurodegeneration.



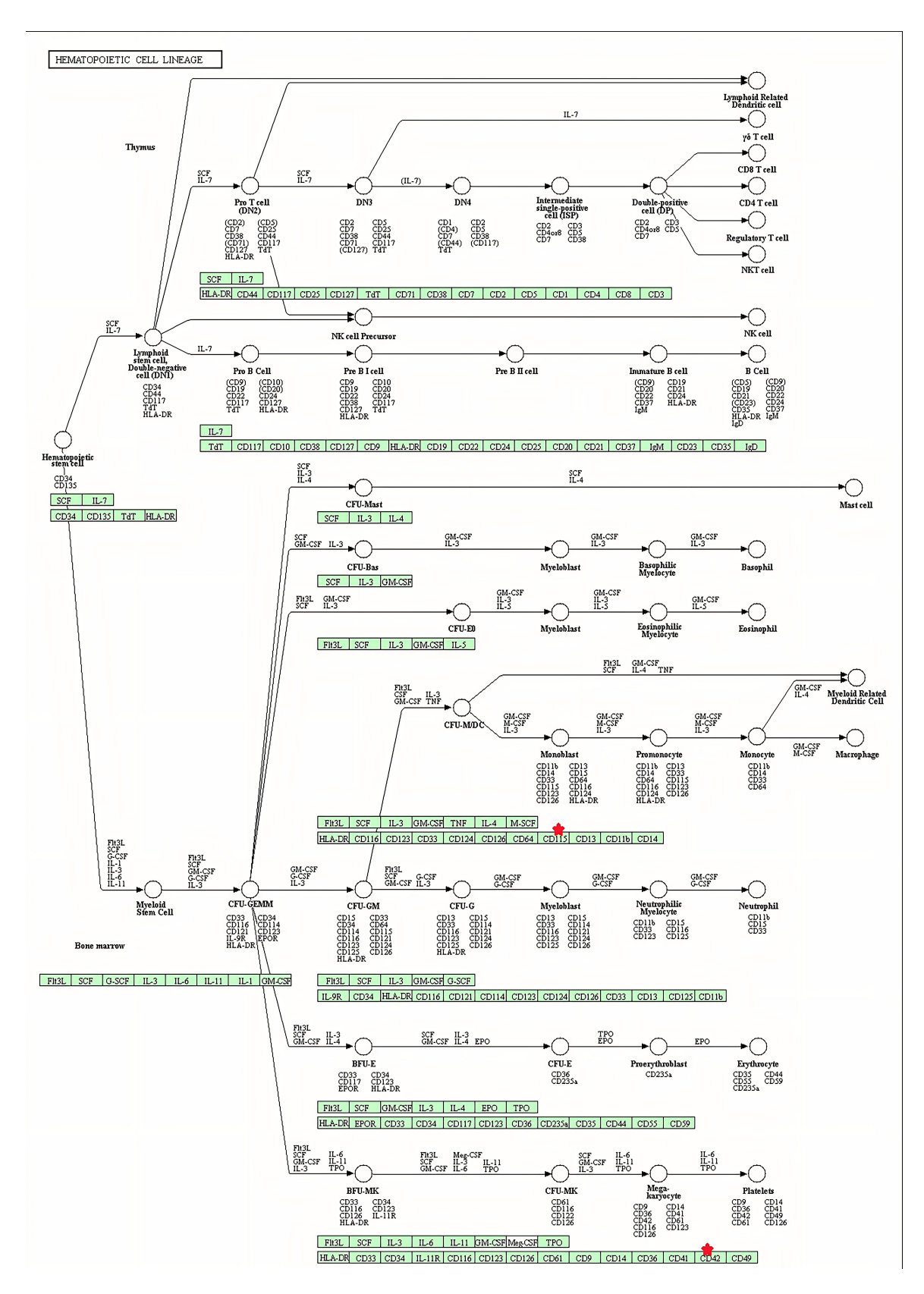


Fig. 9. Differentially expressed proteins are involved in the hematopoietic cell lineage pathway. Red stars represent the proteins identified as differentially expressed between the methamphetamine-dependent and control individuals. The information about all abbreviations can be found at: https://www.genome.jp/pathway/hsa04640 [27].



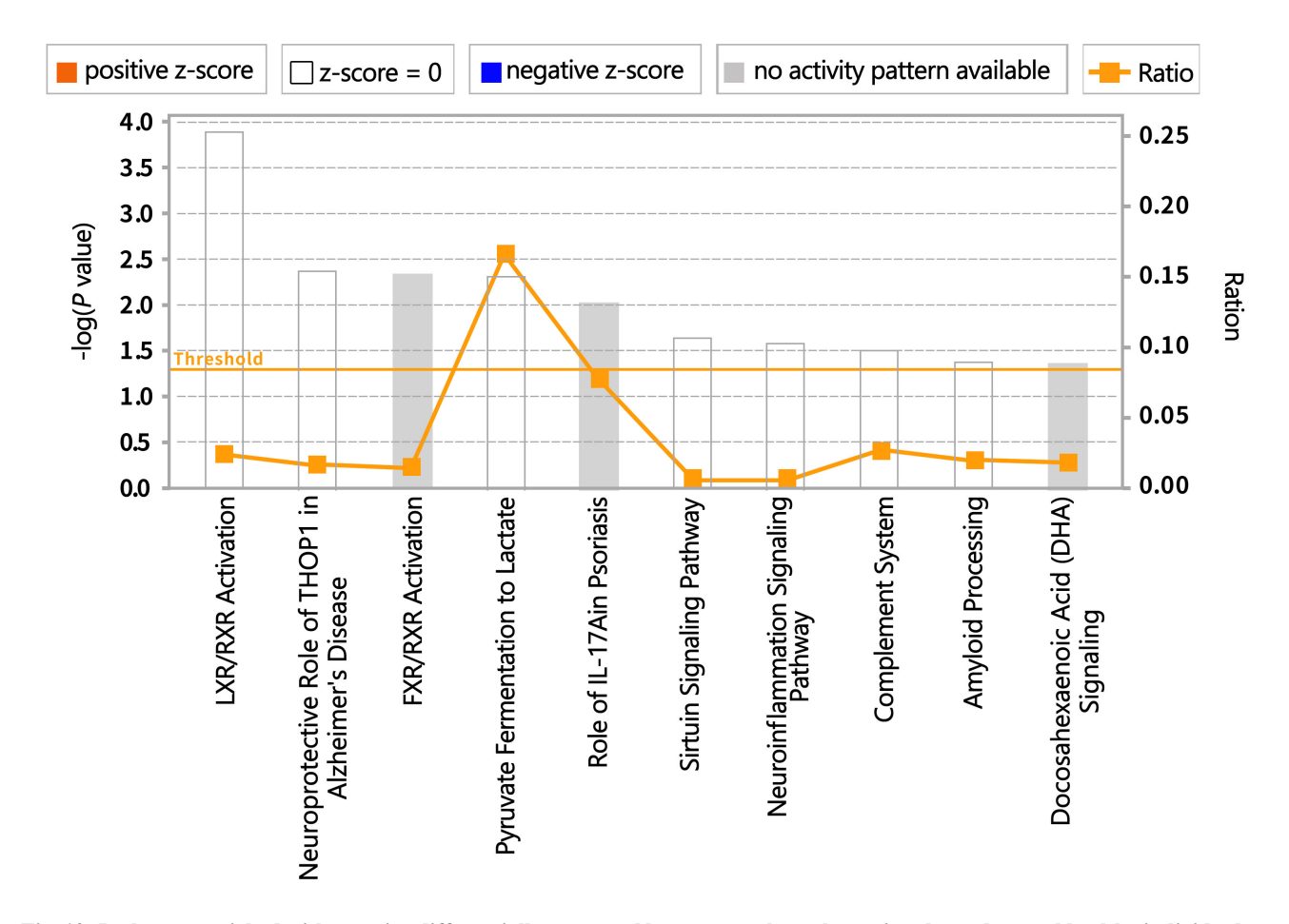


Fig. 10. Pathways enriched with proteins differentially expressed between methamphetamine-dependent and healthy individuals. FXR, farnesoid X receptor; IL, interleukin; LXR, liver X receptor; RXR, retinoid X receptor; THOP1, Thimet Oligopeptidase 1.

Collectively, our findings indicate that METH misuse modulates the expression of proteins such as CETP and APMAP, implicating cardiovascular function and neurodegenerative pathways. The upregulation of CETP is suggestive of an augmented risk for cardiovascular pathology and A $\beta$ -related neurodegenerative processes, whereas the downregulation of APMAP may signal an enhanced progression towards neurodegeneration through increased A $\beta$  accumulation. These proteomic alterations shed light on the systemic ramifications of METH abuse and underscore the imperative for integrated treatment modalities that concurrently tackle the multifaceted repercussions of METH dependency and its extensive health sequelae.

# 4.2 Nervous System-related Proteins

Prolonged stimulation of the nervous system by METH impairs dopaminergic nerve endings and induces neuronal necrosis [37], potentially contributing to the development of PD [10]. Microglia are important neuroimmune cells in the CNS. Following nervous system damage, microglia become activated, releasing neurotrophic factors to repair tissue, engulfing damaged neurons, and promoting repair, thus acting in a neuroprotective capacity [38]. However, in neurodegenerative diseases, overactivated mi-

croglia trigger inflammation and release neuroinflammatory factors, such as nitric oxide, interleukins 6 and  $1\beta$ , and tumor necrosis factor  $\alpha$ , inducing neurotoxicity [12]. Microglia overactivation has been associated with the NF- $\kappa$ B signaling pathway [39].

The present study also found significantly elevated expression of DPP4 and CSF1R in the METH group compared with the healthy control group. CSF1R regulates microglial proliferation and differentiation [40]. DPP4, also known as CD26, is a cell surface serine protease that activates the extracellular signal-regulated kinase 1/2 (ERK1/2)–NF- $\kappa$ B signaling pathway [41]. Because NF- $\kappa$ B can activate microglia, DPP4 may have dual roles: protecting and repairing damaged neurons, while also promoting inflammatory reactions and aggravating damage to the nervous system.

We also observed increased serum LRRTM2 and EFEMP1 protein expression in the METH group. LR-RTM2, a neural cell adhesion molecule containing leucinerich repeats, is involved in neurodevelopmental processes, including axon growth, synapse formation, and axon bundling [42,43]. EFEMP1, an extracellular matrix glycoprotein containing epidermal growth factor-like domains, regulates glial cell development, migration, differentiation, and synaptic proliferation, suggesting roles in nervous sys-



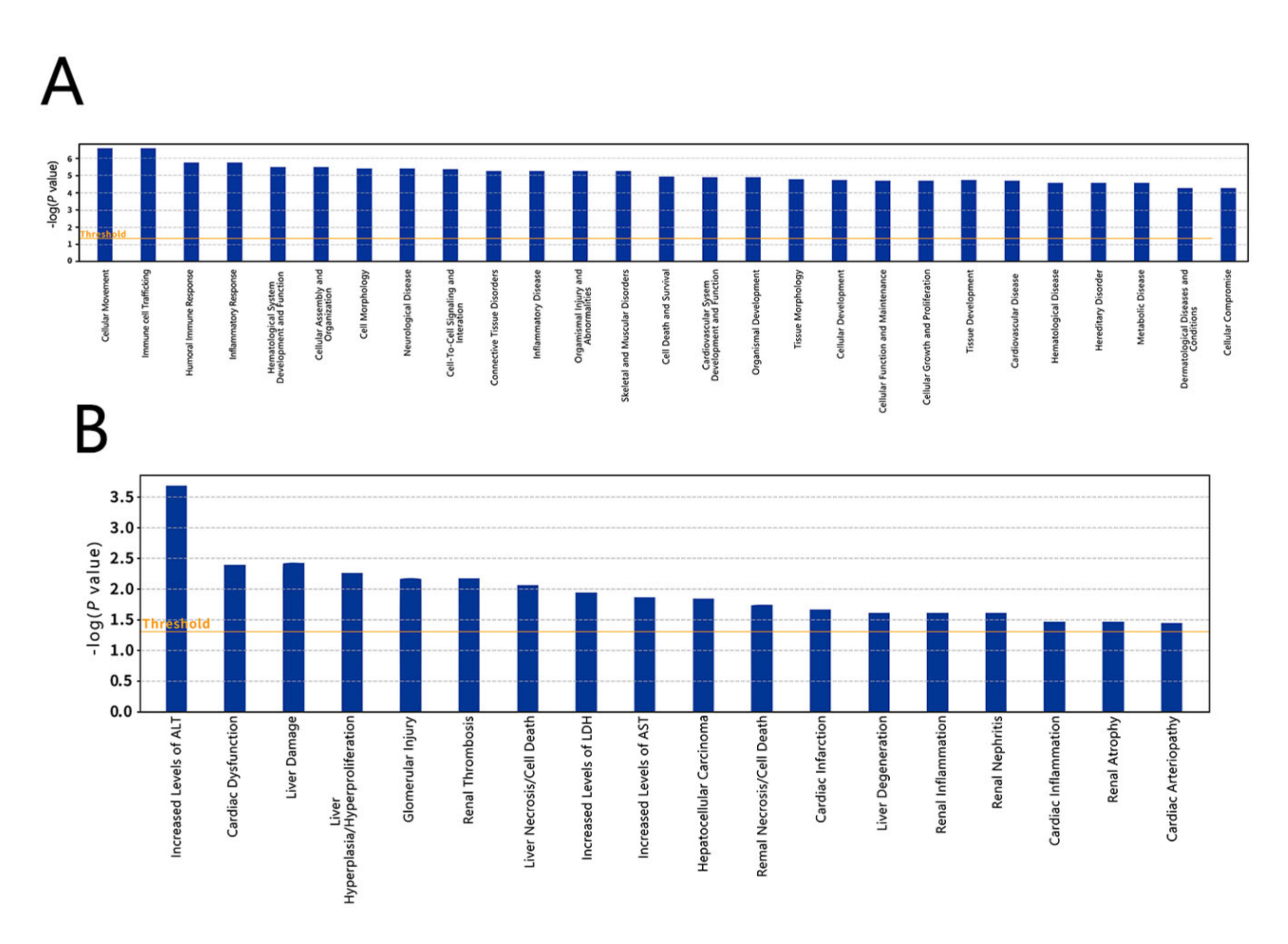


**Fig. 11. Differential expressed protein enrichment results.** (A) Biological functions and diseases enriched in the differentially expressed proteins between methamphetamine-dependent and healthy control individuals. (B) Toxicological types enriched in the differentially expressed proteins.

tem development, learning, and memory [44,45]. While we did not examine the functional effects of elevated LR-RTM2 and EFEMP1 in chronic METH users, it is still reasonable to suspect that these two proteins may contribute to METH-induced neurological changes. These results provide new potential molecular targets for exploring cognitive deficiency in METH users.

## 4.3 Immune Response-related Proteins

Prolonged METH use compromises both the innate and adaptive arms of the immune system, increasing susceptibility to viral and bacterial infections, indicating adverse effects on immune function [46]. Multiple mechanisms likely contribute to METH-induced immunosuppression. First, METH elevates synaptic dopamine, which is metabolized by monoamine oxidase into reactive oxygen species (ROS). This oxidative stress damages DNA, lipids, and proteins, directly impairing immune cell viability [47]. Second, METH inhibits the function of innate immune cells, such as natural killer cells, dendritic cells, monocytes, macrophages, and granulocytes, thereby suppressing front-line defenses against pathogens [48,49]. We found several

differentially expressed immune-related proteins in METH users that may represent compensatory responses to counteract immunosuppression. Immunoglobulin lambda variable 3 (IGLV3)-16, IGLV3-25, and immunoglobulin heavy variable 3-64 showed decreased expression, suggesting impaired antibody production. Meanwhile, immunoglobulin kappa variable 1-6, IGLV6-57, PIGR, C1qA, and ficolin-3 were upregulated, suggesting attempts to boost humoral immunity.

Immunoglobulins are antigen-binding antibody proteins composed of two light chains and two heavy chains. As immune complexes, immunoglobulins can activate the complement cascade. The complement system is an enzymatic cascade that amplifies immunity through classic, alternative, and lectin pathways [50]. Complement activation on pathogen surfaces mediates cell lysis, while split products interact with adaptive immunity [51]. PIGR is a crucial transmembrane glycoprotein receptor that transports immunoglobulins across mucosal epithelial cells into secretions [52]. Each immunoglobulin molecule requires one PIGR molecule for secretion; therefore, PIGR deficiency reduces antibody levels on the mucosal surface. C1q, part

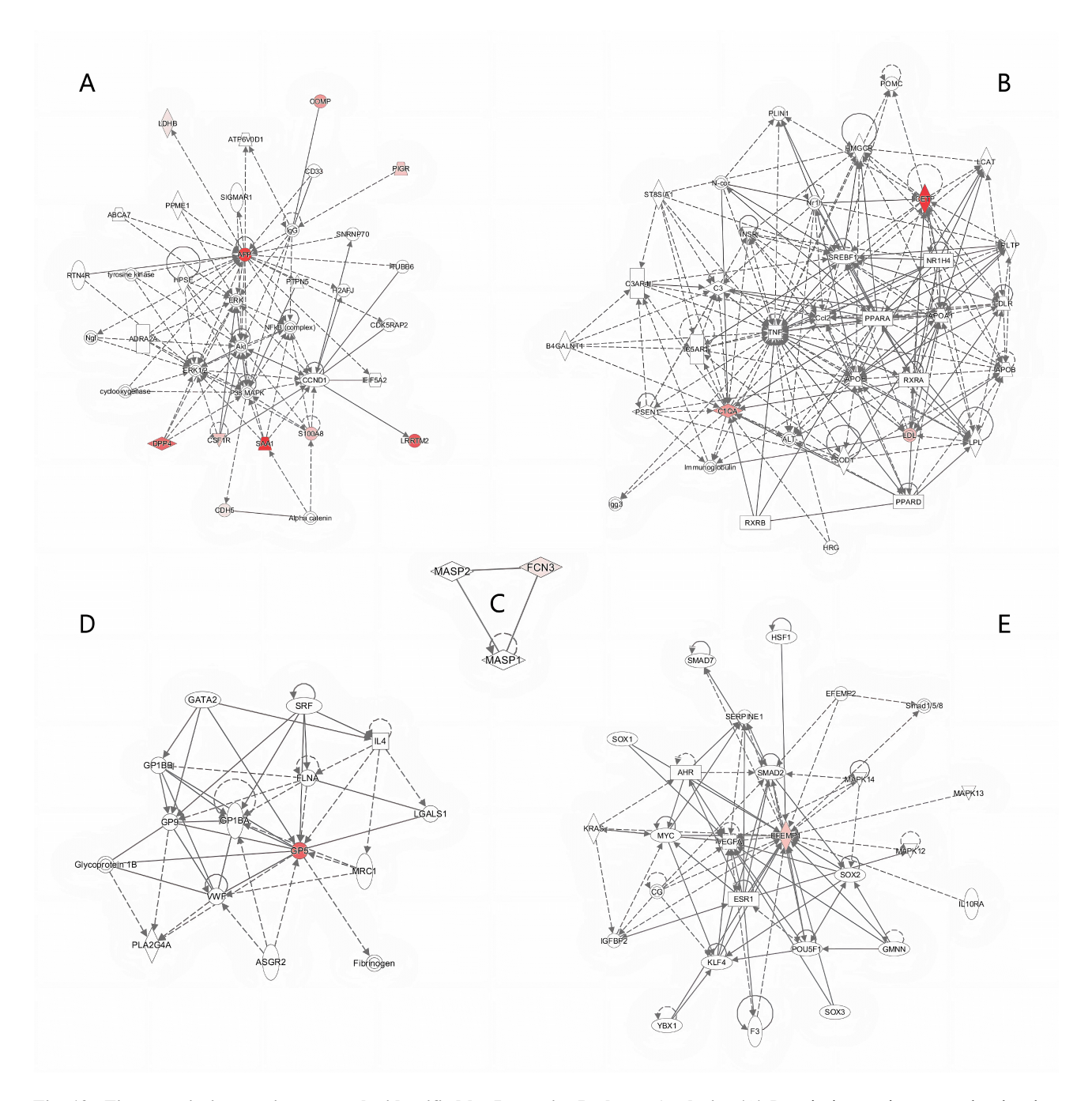


Fig. 12. Five protein interaction networks identified by Ingenuity Pathway Analysis. (A) Protein interaction network related to cellular assembly/organization, metabolic disease, and cellular movement. (B) Protein interaction network related to lipid metabolism, molecular transport, and small molecule biochemistry. (C) Protein interaction network related to immune response, inflammatory response, and cardiovascular disease. (D) Protein interaction network related to connective tissue disorders, hematological disease, and organismal injury and abnormalities. (E) Protein interaction network related to cellular growth, proliferation, cancer, and organismal injury and abnormalities. Colors identify differentially expressed proteins, with color saturation representing the level of protein expression: dark red indicates higher expression, light pink represents lower expression.

of the complement C1 complex, binds immunoglobulin (Immunoglobulin G [IgG] or Immunoglobulin M [IgM]) complexes to trigger the classic pathway. Elevated C1qA in the brain of individuals with AD suggests a pathogenic role [53,54]. Ficolin-3 is a pattern recognition receptor that activates the lectin complement pathway through its

collagen-like and fibrinogen-like domains, contributing to innate pathogen sensing [53,55]. The differential expression of these immune-related proteins indicates that METH-induced dysfunction provokes compensatory responses to bolster both innate and adaptive immunity against infections. However, more research is needed to fully eluci-



date the mechanisms of METH-induced immunosuppression and compensatory immune protein expression. Additionally, the discovery of differentially expressed immunerelated proteins in METH users may inform the creation of targeted immunomodulatory treatments. Such therapies would aim to recalibrate the immune equilibrium, mitigating the increased vulnerability to infectious diseases observed among individuals with METH dependence.

#### 4.4 Energy Metabolism-related Proteins

METH directly enters neuronal mitochondria through its lipophilic properties, impairing the respiratory chain and disrupting cellular energy metabolism. Brain function maintenance requires substantial energy input, and therefore METH-induced energy deficits can promote neuronal death and neurodegenerative diseases [56,57].

Lactate dehydrogenase (LDH) interconverts pyruvate and lactate, participating in cellular anaerobic respiration [58]. In AD models, early stage neuronal lactate dehydrogenase (LDHA) upregulation reduces mitochondrial activity and ROS production, conferring  $A\beta$  toxicity resistance and improving survival [59]. However, late stage LDHA downregulation shunts pyruvate into mitochondria, elevating ROS and apoptosis, impairing cognition. In our study, LDHB was upregulated in the METH group, possibly an adaptive response similar to early AD, countering  $A\beta/ROS$  by supplementing anaerobic Adenosine Triphosphate (ATP) generation upon METH-induced respiratory damage. However, LDHB upregulation may also reflect a shift toward aerobic glycolysis and reduced mitochondrial pyruvate metabolism. Further research is required to determine whether LDHB upregulation is beneficial or maladaptive, and to elucidate effects across cell types. Nonetheless, our data indicate perturbed energy homeostasis in METHinduced neurodegeneration.

# 4.5 Calcium-binding and Regulation-related Proteins

Calcium is a key intracellular messenger regulating neuronal functions such as long-term potentiation, neuronal perception, synaptic plasticity, and cell proliferation [60]. Calcium dysregulation can promote neurodegeneration [61,62]. The calcium-binding protein S100A8 mediates inflammatory/oxidative stress responses. Its expression in immune cells is stimulated by nerve injury, eliciting neuroinflammation [63]. Cadherin-5 (CDH5) is a calcium-dependent cell adhesion glycoprotein involved in cell recognition, migration, and tissue morphogenesis. Cadherin expression is developmentally regulated, including N-cadherin enrichment in developing neurons [64]. We found that S100A8 and CDH5 were upregulated in the METH-dependent group. This may represent adaptive responses, with S100A8 counteracting drug-induced calcium perturbations and neuroinflammation, while CDH5 promotes structural plasticity repairing neuronal damage.

It is worth mentioning that, unlike in rodent models, serum represents a minimally invasive human sample. The association between changes in serum proteins and cognitive impairments suggests that the systemic effects of METH extend beyond the blood-brain barrier, manifesting as peripheral biomarkers that may reflect concurrent changes in the CNS [65]. This implies that METH's systemic impact transcends the blood-brain barrier. Serum proteins can be utilized for the early detection and monitoring of the progression of neurodegenerative diseases associated with METH abuse. For instance, the observed increase in serum levels of APP in this study potentially signals an elevated risk of amyloid plaque formation. Similarly, changes in serum levels of proteins such as CETP and APMAP may indicate underlying neuropathological processes. The differential expression of these genes in serum likely indicates a systemic response to METH's neurotoxi-

# 5. Study Limitations

While the sample size of this study may appear small, it is noteworthy that previous investigations employing the same label-free proteomics methodology have similarly focused on selected subpopulations, such as individuals with schizophrenia or cancer. In such prior studies, the sample sizes for the specialized groups were often lower than 20 [66–68], yet they yielded statistically significant findings regarding alterations in serum protein expression. Consequently, the inclusion of 12 participants with METH dependence in our present study can be deemed sufficient to substantiate our research findings. In addition, the functions of the proteins exhibiting differential expression in individuals with METH dependence have been discussed herein. Nevertheless, owing to the limited number of participants in this study, it is imperative to validate the findings on a broader scale by recruiting a larger cohort of individuals with METH addiction.

#### 6. Conclusions

In summary, our serum proteomic analysis revealed numerous DEPs between individuals with METH dependence and health individuals. The identified proteins were involved in cognitive dysfunction, nervous system inflammation and disease, immune response, energy metabolism, and calcium binding and regulation. These expression changes likely reflect molecular adaptions underlying METH-induced damage to the nervous, immune, and metabolic systems. Further exploration of the functional roles of these DEPs will provide insights into the molecular mechanisms of METH dependence. Elucidating the involvement of these proteins in the brain's response to chronic METH exposure will also reveal novel targets for the prevention and treatment of METH addiction. Thus, overall, this proteomic profile highlights candidate mediators of the systemic effects of long-term METH use, point-



ing toward new avenues for understanding the biological basis of dependence and for developing targeted therapeutics.

# Availability of Data and Materials

The data sets generated and analyzed during the current study are available in the ProteomeXchange Consortium (http://proteomecentral.proteomexchange.org) via the iProX partner repository with the dataset identifier PXD040112.

# **Author Contributions**

YW, CZ and CL were responsible for the study concept and design. CZ is responsible for Funding acquisition. YZ contributed to the collection of participate serum and data curation. YL performed the proteomics analysis. LL contributed to conducting the literature searches. XW contributed to interpreting the data. Furthermore, both LL and XW were involved in drafting the manuscript, with XW providing the final approval for the version to be published. HW was responsible for designing and editing images and tables for this article. YW, CZ and CL provided critical revision of the manuscript for important intellectual content. All authors contributed to editorial changes in the manuscript. All authors read and approved the final manuscript. All authors have participated sufficiently in the work and agreed to be accountable for all aspects of the work.

#### **Ethics Approval and Consent to Participate**

This study was approved by the Ethics Committee of Shanghai University of Sport (No. 102772019RT044) and conducted in accordance with the Helsinki Declaration of 1975. All participant information remained confidential, and all patients provided written informed consent.

#### Acknowledgment

We thank the Shiliping Compulsory Isolation Detoxification Center in Zhejiang Province for collecting basic information and serum samples.

#### **Funding**

This work was supported by the National Social Science Fund of China (No. 17ZDA330).

#### **Conflict of Interest**

The authors declare no conflict of interest.

## **Supplementary Material**

Supplementary material associated with this article can be found, in the online version, at https://doi.org/10.31083/j.jin2305107.

#### References

- [1] Drug Enforcement Administration. 2007. Available at: https://www.dea.gov (Accessed: 13 March 2022).
- [2] Chomchai C, Chomchai S. Global patterns of methamphetamine use. Current Opinion in Psychiatry. 2015; 28: 269–274.
- [3] Potvin S, Pelletier J, Grot S, Hébert C, Barr AM, Lecomte T. Cognitive deficits in individuals with methamphetamine use disorder: A meta-analysis. Addictive Behaviors. 2018; 80: 154–160
- [4] Krasnova IN, Justinova Z, Cadet JL. Methamphetamine addiction: involvement of CREB and neuroinflammatory signaling pathways. Psychopharmacology. 2016; 233: 1945–1962.
- [5] London ED, Kohno M, Morales AM, Ballard ME. Chronic methamphetamine abuse and corticostriatal deficits revealed by neuroimaging. Brain Research. 2015; 1628: 174–185.
- [6] Cuomo I, Motta P, Fini C, Kotzalidis GD, De Filippis S. The Efficacy of Asenapine in the Treatment of Bipolar Disorder: a Naturalistic Longitudinal Study Indicating a Favourable Response in Patients with Substance Abuse Comorbidity. European Psychiatry. 2015, 30: 1152.
- [7] Jackson AR, Shah A, Kumar A. Methamphetamine alters the normal progression by inducing cell cycle arrest in astrocytes. PloS One. 2014; 9: e109603.
- [8] Yamamoto BK, Moszczynska A, Gudelsky GA. Amphetamine toxicities: classical and emerging mechanisms. Annals of the New York Academy of Sciences. 2010; 1187: 101–121.
- [9] Arida RM, Gomes da Silva S, de Almeida AA, Cavalheiro EA, Zavala-Tecuapetla C, Brand S, et al. Differential effects of exercise on brain opioid receptor binding and activation in rats. Journal of Neurochemistry. 2015; 132: 206–217.
- [10] Hiebert NM, Seergobin KN, Vo A, Ganjavi H, MacDonald PA. Dopaminergic therapy affects learning and impulsivity in Parkinson's disease. Annals of Clinical and Translational Neurology. 2014; 1: 833–843.
- [11] Polvat T, Prasertporn T, Na Nakorn P, Pannengpetch S, Suwanjang W, Panmanee J, et al. Proteomic Analysis Reveals the Neurotoxic Effects of Chronic Methamphetamine Self-Administration-Induced Cognitive Impairments and the Role of Melatonin-Enhanced Restorative Process during Methamphetamine Withdrawal. Journal of Proteome Research. 2023; 22: 3348–3359.
- [12] Kingwell K. Neurodegenerative disease: Microglia in early disease stages. Nature Reviews. Neurology. 2012; 8: 475.
- [13] Park JH, Seo YH, Jang JH, Jeong CH, Lee S, Park B. Asiatic acid attenuates methamphetamine-induced neuroinflammation and neurotoxicity through blocking of NF-kB/STAT3/ERK and mitochondria-mediated apoptosis pathway. Journal of Neuroinflammation. 2017; 14: 240.
- [14] Kong D, Mao JH, Li H, Wang JY, Li YY, Wu XC, et al. Effects and associated transcriptomic landscape changes of methamphetamine on immune cells. BMC Medical Genomics. 2022; 15: 144
- [15] Nazari A, Zahmatkesh M, Mortaz E, Hosseinzadeh S. Effect of methamphetamine exposure on the plasma levels of endothelialderived microparticles. Drug and Alcohol Dependence. 2018; 186: 219–225.
- [16] Maskell PD, Albeishy M, De Paoli G, Wilson NE, Seetohul LN. Postmortem redistribution of the heroin metabolites morphine and morphine-3-glucuronide in rabbits over 24 h. International Journal of Legal Medicine. 2016; 130: 519–531.
- [17] Zhu L, Li J, Dong N, Guan F, Liu Y, Ma D, et al. mRNA changes in nucleus accumbens related to methamphetamine addiction in mice. Scientific Reports. 2016; 6: 36993.
- [18] USAn Psychiatric Association. Diagnostic and statistical manual of mental disorders. 5th edn. USAn Psychiatric Publishing:



- Arlington, VA. 2013.
- [19] Thermo Fisher Scientific. Xcalibur software. 2022. Available at: https://www.thermofisher.com/order/catalog/product/OPT ON-30965?SID=srch-srp-OPTON-30965 (Accessed: 3 March 2023).
- [20] Cox J, Mann M. MaxQuant enables high peptide identification rates, individualized p.p.b.-range mass accuracies and proteomewide protein quantification. Nature Biotechnology. 2008; 26: 1367–1372.
- [21] MetaboAnalyst software. 2017. Available at: https://www.metaboanalyst.ca/ (Accessed: 15 April 2017).
- [22] Saeed AI, Sharov V, White J, Li J, Liang W, Bhagabati N, et al. TM4: a free, open-source system for microarray data management and analysis. BioTechniques. 2003; 34: 374–378.
- [23] MathWorks. MATLAB (Version R2019b). 2019. Available at: https://www.mathworks.com (Accessed: 14 April 2019).
- [24] Umetrics. SIMCA 14.1. 2018. Available at: https://www.sartorius.com/en/products/process-analytical-technology/data-analytics-software/simca (Accessed: 23 August 2018).
- [25] IBM Corp. IBM SPSS Statistics for Windows, Version 24.0. 2017. Available at: https://www.ibm.com/products/spss-statistics (Accessed: 23 August 2018).
- [26] Ingenuity Pathway Analysis (IPA) software. 2018. Available at: https://digitalinsights.qiagen.com/IPA (Accessed: 23 August 2018).
- [27] Kanehisa M, Furumichi M, Sato Y, Kawashima M, Ishiguro-Watanabe M. KEGG for taxonomy-based analysis of pathways and genomes. Nucleic Acids Research. 2023; 51: D587–D592.
- [28] Garwood ER, Bekele W, McCulloch CE, Christine CW. Amphetamine exposure is elevated in Parkinson's disease. Neurotoxicology. 2006; 27: 1003–1006.
- [29] Eimer WA, Vijaya Kumar DK, Navalpur Shanmugam NK, Rodriguez AS, Mitchell T, Washicosky KJ, et al. Alzheimer's Disease-Associated β-Amyloid Is Rapidly Seeded by Herpesviridae to Protect against Brain Infection. Neuron. 2018; 99: 56–63.e3.
- [30] Bergström P, Agholme L, Nazir FH, Satir TM, Toombs J, Wellington H, et al. Amyloid precursor protein expression and processing are differentially regulated during cortical neuron differentiation. Scientific Reports. 2016; 6: 29200.
- [31] Kasai T, Tokuda T, Taylor M, Kondo M, Mann DMA, Foulds PG, et al. Correlation of Aβ oligomer levels in matched cerebrospinal fluid and serum samples. Neuroscience Letters. 2013; 551: 17–22.
- [32] Rice HC, de Malmazet D, Schreurs A, Frere S, Van Molle I, Volkov AN, et al. Secreted amyloid-β precursor protein functions as a GABA\_BR1a ligand to modulate synaptic transmission. Science (New York, N.Y.). 2019; 363: eaao4827.
- [33] Mizoguchi H, Yamada K. Methamphetamine use causes cognitive impairment and altered decision-making. Neurochemistry International. 2019; 124: 106–113.
- [34] Shukla M, Vincent B. The multi-faceted impact of methamphetamine on Alzheimer's disease: From a triggering role to a possible therapeutic use. Ageing Research Reviews. 2020; 60: 101062.
- [35] Gamba P, Testa G, Sottero B, Gargiulo S, Poli G, Leonarduzzi G. The link between altered cholesterol metabolism and Alzheimer's disease. Annals of the New York Academy of Sciences. 2012; 1259: 54–64.
- [36] Mosser S, Alattia JR, Dimitrov M, Matz A, Pascual J, Schneider BL, *et al*. The adipocyte differentiation protein APMAP is an endogenous suppressor of  $A\beta$  production in the brain. Human Molecular Genetics. 2015; 24: 371–382.
- [37] Mott RT, Ait-Ghezala G, Town T, Mori T, Vendrame M, Zeng J, *et al.* Neuronal expression of CD22: novel mechanism for in-

- hibiting microglial proinflammatory cytokine production. Glia. 2004; 46: 369–379.
- [38] Perry VH, Nicoll JAR, Holmes C. Microglia in neurodegenerative disease. Nature Reviews. Neurology. 2010; 6: 193–201.
- [39] Gong QH, Pan LL, Liu XH, Wang Q, Huang H, Zhu YZ. S-propargyl-cysteine (ZYZ-802), a sulphur-containing amino acid, attenuates beta-amyloid-induced cognitive deficits and pro-inflammatory response: involvement of ERK1/2 and NF-κB pathway in rats. Amino Acids. 2011; 40: 601–610.
- [40] Elmore MRP, Najafi AR, Koike MA, Dagher NN, Spangenberg EE, Rice RA, et al. Colony-stimulating factor 1 receptor signaling is necessary for microglia viability, unmasking a microglia progenitor cell in the adult brain. Neuron. 2014; 82: 380–397.
- [41] Wronkowitz N, Görgens SW, Romacho T, Villalobos LA, Sánchez-Ferrer CF, Peiró C, et al. Soluble DPP4 induces inflammation and proliferation of human smooth muscle cells via protease-activated receptor 2. Biochimica et Biophysica Acta. 2014; 1842: 1613–1621.
- [42] Anderson NE, Somaratne J, Mason DF, Holland D, Thomas MG. Neurological and systemic complications of tuberculous meningitis and its treatment at Auckland City Hospital, New Zealand. Journal of Clinical Neuroscience: Official Journal of the Neurosurgical Society of Australasia. 2010; 17: 1114–1118.
- [43] Pandian JD, Thomas SV, Santoshkumar B, Radhakrishnan K, Sarma PS, Joseph S, et al. Epilepsia partialis continua—a clinical and electroencephalography study. Seizure. 2002; 11: 437–441.
- [44] Ulrich R, Imbschweiler I, Kalkuhl A, Lehmbecker A, Ziege S, Kegler K, *et al.* Transcriptional profiling predicts overwhelming homology of Schwann cells, olfactory ensheathing cells, and Schwann cell-like glia. Glia. 2014; 62: 1559–1581.
- [45] Vukovic J, Marmorstein LY, McLaughlin PJ, Sasaki T, Plant GW, Harvey AR, et al. Lack of fibulin-3 alters regenerative tissue responses in the primary olfactory pathway. Matrix Biology: Journal of the International Society for Matrix Biology. 2009; 28: 406–415.
- [46] Prakash MD, Tangalakis K, Antonipillai J, Stojanovska L, Nurgali K, Apostolopoulos V. Methamphetamine: Effects on the brain, gut and immune system. Pharmacological Research. 2017; 120: 60–67.
- [47] Cadet JL, Brannock C. Free radicals and the pathobiology of brain dopamine systems. Neurochemistry International. 1998; 32: 117–131.
- [48] Liu X, Silverstein PS, Singh V, Shah A, Qureshi N, Kumar A. Methamphetamine increases LPS-mediated expression of IL-8, TNF-α and IL-1β in human macrophages through common signaling pathways. PloS One. 2012; 7: e33822.
- [49] Loftis JM, Choi D, Hoffman W, Huckans MS. Methamphetamine causes persistent immune dysregulation: a crossspecies, translational report. Neurotoxicity Research. 2011; 20: 59–68.
- [50] Kouser L, Madhukaran SP, Shastri A, Saraon A, Ferluga J, Al-Mozaini M, et al. Emerging and Novel Functions of Complement Protein C1q. Frontiers in Immunology. 2015; 6: 317.
- [51] Stephan AH, Madison DV, Mateos JM, Fraser DA, Lovelett EA, Coutellier L, et al. A dramatic increase of C1q protein in the CNS during normal aging. The Journal of Neuroscience: the Official Journal of the Society for Neuroscience. 2013; 33: 13460– 13474.
- [52] Turula H, Wobus CE. The Role of the Polymeric Immunoglobulin Receptor and Secretory Immunoglobulins during Mucosal Infection and Immunity. Viruses. 2018; 10: 237.
- [53] Fonseca MI, Kawas CH, Troncoso JC, Tenner AJ. Neuronal localization of C1q in preclinical Alzheimer's disease. Neurobiology of Disease. 2004; 15: 40–46.
- [54] Zhou J, Fonseca MI, Pisalyaput K, Tenner AJ. Complement C3 and C4 expression in C1q sufficient and deficient mouse models



- of Alzheimer's disease. Journal of Neurochemistry. 2008; 106: 2080–2092.
- [55] Skjoedt MO, Palarasah Y, Munthe-Fog L, Jie Ma Y, Weiss G, Skjodt K, et al. MBL-associated serine protease-3 circulates in high serum concentrations predominantly in complex with Ficolin-3 and regulates Ficolin-3 mediated complement activation. Immunobiology. 2010; 215: 921–931.
- [56] Kapogiannis D, Mattson MP. Disrupted energy metabolism and neuronal circuit dysfunction in cognitive impairment and Alzheimer's disease. The Lancet. Neurology. 2011; 10: 187– 198.
- [57] Zheng B, Liao Z, Locascio JJ, Lesniak KA, Roderick SS, Watt ML, et al. PGC-1α, a potential therapeutic target for early intervention in Parkinson's disease. Science Translational Medicine. 2010; 2: 52ra73.
- [58] Burgner JW II, Ray WJ Jr. On the origin of the lactate dehydrogenase induced rate effect. Biochemistry. 1984; 23: 3636–3648.
- [59] Newington JT, Rappon T, Albers S, Wong DY, Rylett RJ, Cumming RC. Overexpression of pyruvate dehydrogenase kinase 1 and lactate dehydrogenase A in nerve cells confers resistance to amyloid  $\beta$  and other toxins by decreasing mitochondrial respiration and reactive oxygen species production. The Journal of Biological Chemistry. 2012; 287: 37245–37258.
- [60] Srivastava U, Aromolaran AS, Fabris F, Lazaro D, Kassotis J, Qu Y, et al. Novel function of α<sub>1</sub>D L-type calcium channel in the atria. Biochemical and Biophysical Research Communications. 2017; 482: 771–776.
- [61] Mitaeva YI, Mozherov AM, Kastalskiy IA, Mishchenko TA, Mukhina IV. Intracellular Calcium Network Activity in the Hippocampus CA3 Region in Rat Postnatal Development. Sovre-

- mennye Tehnologii v Medicine. 2016; 8: 167-177.
- [62] Saddouk FZ, Ginnan R, Singer HA. Ca<sup>2+</sup>/Calmodulin-Dependent Protein Kinase II in Vascular Smooth Muscle. Advances in Pharmacology (San Diego, Calif.). 2017; 78: 171– 202
- [63] Chernov AV, Dolkas J, Hoang K, Angert M, Srikrishna G, Vogl T, et al. The calcium-binding proteins S100A8 and S100A9 initiate the early inflammatory program in injured peripheral nerves. The Journal of Biological Chemistry. 2015; 290: 11771–11784.
- [64] Redies C. Cadherins in the central nervous system. Progress in Neurobiology. 2000; 61: 611–648.
- [65] Janigro D, Bailey DM, Lehmann S, Badaut J, O'Flynn R, Hirtz C, et al. Peripheral Blood and Salivary Biomarkers of Blood-Brain Barrier Permeability and Neuronal Damage: Clinical and Applied Concepts. Frontiers in Neurology. 2021; 11: 577312.
- [66] Li Y, Zhou K, Zhang Z, Sun L, Yang J, Zhang M, et al. Label-free quantitative proteomic analysis reveals dysfunction of complement pathway in peripheral blood of schizophrenia patients: evidence for the immune hypothesis of schizophrenia. Molecular BioSystems. 2012; 8: 2664–2671.
- [67] Sun Y, Chu JZ, Geng JR, Guan FL, Zhang SC, Ma YC, et al. Label-free based quantitative proteomics analysis to explore the molecular mechanism of gynecological cold coagulation and blood stasis syndrome. Anatomical Record (Hoboken, N.J.: 2007). 2023; 306: 3033–3049.
- [68] Verathamjamras C, Chantaraamporn J, Sornprachum T, Mutapat P, Chokchaichamnankit D, Mingkwan K, et al. Label-free quantitative proteomics reveals aberrant expression levels of LRG, C9, FN, A1AT and AGP1 in the plasma of patients with colorectal cancer. Clinical Proteomics. 2023; 20: 15.

